Muscarinic modulation of erg potassium current

Wiebke Hirdes, Lisa F. Horowitz and Bertil Hille

Department of Physiology and Biophysics, University of Washington School of Medicine, Seattle, WA 98195, USA

We studied modulation of current in human embryonic kidney tsA-201 cells coexpressing rat erg1 channels with M_1 muscarinic receptors. Maximal current was inhibited 30% during muscarinic receptor stimulation, with a small positive shift of the midpoint of activation. Inhibition was attenuated by coexpression of the regulator of G-protein signalling RGS2 or of a dominant-negative protein, G_q, but not by *N*-ethylmaleimide or C3 toxin. Overexpression of a constitutively active form of G_q (but not of G_{13} or of G_s) abolished the erg current. Hence it is likely that $G_{q/11}$, and not $G_{i/o}$ or G_{13}, mediates muscarinic inhibition. Muscarinic suppression of erg was attenuated by chelating intracellular Ca^{2+} to < 1 nM free Ca^{2+} with 20 mM BAPTA in the pipette, but suppression was normal if internal Ca^{2+} was strongly clamped to a 129 nM free Ca^{2+} level with a BAPTA buffer and this was combined with numerous other measures to prevent intracellular Ca^{2+} transients (pentosan polysulphate, preincubation with thapsigargin, and removal of extracellular Ca^{2+}). Hence a minimum amount of Ca^{2+} was necessary for the inhibition, but a Ca^{2+} elevation was not. The ATP analogue AMP-PCP did not prevent inhibition. The protein kinase C (PKC) blockers staurosporine and bisindolylmaleimide I did not prevent inhibition, and the PKC-activating phorbol ester PMA did not mimic it. Neither the tyrosine kinase inhibitor genistein nor the tyrosine phosphatase inhibitor dephostatin prevented inhibition by oxotremorine-M. Hence protein kinases are not needed. Experiments with a high concentration of wortmannin were consistent with recovery being partially dependent on PIP_2 resynthesis. Wortmannin did not prevent muscarinic inhibition. Our studies of muscarinic inhibition of erg current suggest a role for phospholipase C, but not the classical downstream messengers, such as PKC or a calcium transient.

(Received 23 April 2004; accepted after revision 28 June 2004; first published online 2 July 2004)
Corresponding author B. Hille: Department of Physiology and Biophysics, University of Washington School of Medicine, G-424 Health Sciences Building, Box 357290, Seattle, WA 98195-7290, USA. Email: hille@u.washington.edu

The ether-à-go-go-related gene (erg) channel belongs to the family of ether-à-go-go (EAG) K^+ channels. The human erg1 (HERG) is the molecular correlate of the rapidly activating component (I_{Kr}) of the delayed rectifier current in the heart (Warmke & Ganetzky, 1994; Sanguinetti *et al.* 1995; Trudeau *et al.* 1995). This channel has been of particular medical interest because HERG plays a critical role in cardiac rhythmicity and mutations of the erg gene are one cause of long QT syndrome (Curran *et al.* 1995). Erg mRNA is expressed in multiple brain regions (Saganich *et al.* 2001) and in many other parts of the body (Wymore *et al.* 1997; Shi *et al.* 1997). Blockade of erg current by a variety of pharmacological agents, e.g. antihistamines (Zhou *et al.* 1999), antipsychotics (Rampe *et al.* 1998), antiarrhythmics (Kiehn *et al.* 1995) and psychoactive drugs like ethanol, cocaine (Karle & Kiehn, 2002) and nicotine (Satoh, 2002), can contribute to life-threatening arrhythmias.

Erg currents rectify inwardly. However, in contrast to members of the inwardly rectifying Kir channel family, the rectification is caused by atypical biophysical properties of two gates: a slow activation gate and a rapid inactivation gate (Shibasaki, 1987). The slow activation gate leads to the slow current activation seen at positive potentials, e.g. the delayed rectifier current (I_{Kr}) in the heart. The slowness of the reverse process, deactivation, combined with rapid removal of inactivation, allows a large transient tail current to flow during membrane hyperpolarization, as seen in the repolarizing phase of the cardiac action potential. Increasing steady-state inactivation at positive potentials underlies inward rectification and prevents loss of K^+ during prolonged depolarizations. For a review of the biophysics of the erg channel see Tristani-Firouzi & Sanguinetti (2003). Subtle modulation of these biophysical properties by second-messenger pathways can lead to dramatic alterations in the functional

W. Hirdes and L. F. Horowitz contributed equally to this work

DOI: 10.1113/jphysiol.2004.066944

behaviour of excitable cells (reviewed in Bauer & Schwarz, 2001).

Erg1 and KCNQ2/3 K^+ channels both contribute to M-like K^+ currents (Selyanko *et al.* 1999; Meves *et al.* 1999), and are suppressed by the G_q-coupled M_1-muscarinic receptor (M_1R) in NG108-15 mouse neuroblastoma × rat glioma cells (Selyanko *et al.* 1999; Higashida *et al.* 2000). Many brain regions have overlapping expression of erg and KCNQ2/3, consistent with the possibility that erg could be an important component of M-like currents in the brain (Saganich *et al.* 2001). In the heart, a recent study suggests the coassembly of erg with KCNQ1, mimicking I_{Kr} (Ehrlich *et al.* 2004). As with KCNQ2/3, muscarinic inhibition of erg current would increase the excitability of cells. Erg currents have been found in an increasing number of cells, including pancreatic β-cells (Rosati *et al.* 2000), chromaffin cells (Gullo *et al.* 2003), pituitary lactotropes (Bauer *et al.* 1999), cerebellar Purkinje neurones (Sacco *et al.* 2003), and brain-stem neurones (Schwarz *et al.* 2003). Since erg currents can be modulated by several G protein-coupled receptors (Bauer *et al.* 1990; Selyanko *et al.* 1999; Schledermann *et al.* 2001), they can have an important role in controlling cellular excitability.

The main signalling pathway of the M_1 muscarinic receptor is activation of phospholipase C-β (PLC_β) by coupling to G_q. PLC_β hydrolyses phosphatidyl inositol 4,5-bisphosphate (PIP_2) into inositol 1,4,5-trisphosphate (IP_3) and 1,2-diacylglycerol (DAG) (Berstein *et al.* 1992). Whereas IP_3 quickly evokes a transient Ca^{2+} increase by release from the endoplasmic reticulum, DAG can trigger several longer lasting slow effects, including activation of protein kinase C (PKC). These pathways affect many ion channels.

Here we characterize the suppression of rat erg1 (erg) by a muscarinic agonist, oxotremorine-M (oxo-M), in tsA cells that have been cotransfected with erg, the M_1R, and green fluorescent protein. We find that muscarinic inhibition of erg current uses $G_{q/11}$ and shares some similarities to inhibition of KCNQ2/3 current, such as dependence on a minimum Ca^{2+} concentration and independence of protein kinases and ATP. In analogy to the modulation of KCNQ2/3 current by depletion and resynthesis of PIP_2 (Suh & Hille, 2002; Zhang *et al.* 2003), it is possible that some portion of the modulation of erg depends on changes of PIP_2, but further evidence is needed.

Methods

Cell culture and transfection

Human tsA-201 (tsA) cells were transiently transfected using Lipofectamine 2000 according to the manufacturer's instructions (Invitrogen, Carlsbad, CA, USA) with the following cDNAs: 1 μg of the rat erg1 (Kv11.1) (kindly provided by Iris Wulfsen, University of Hamburg, Germany), 1 μg of the M_1 muscarinic receptor (M_1R; kindly provided by Neil Nathanson, University of Washington, USA) or of the M_3 muscarinic receptor (kindly provided by Tom Bonner, NIH, USA), and 0.1 μg of green fluorescent protein to serve as a marker for transfection. When indicated, we added 2 μg of one of the following cDNAs: wild-type calmodulin (wtCaM) or dominant-negative calmodulin (dnCaM, both a kind gift from Mark Shapiro, University of Texas Health Science Center at San Antonio, USA; see Geiser *et al.* 1991), constitutively active G_q(Q209L), G_{11}(Q209L), G_{13}(Q226L), $G_s$short (Q213L), dominant-negative G_q(Q209L/D277N), G_{13}(Q226L/D294N), or wild-type RGS2 protein (Guthrie cDNA Resource Center, Guthrie Research Institute, Sayre, PA, USA). For confocal experiments, cells were transfected with the following cDNAs: 1 μg of M_1R and 0.25 μg of the fluorescent probe PKC-C1-EGFP cDNA (kindly provided by Tobias Meyer, Stanford University, USA). Electrophysiology was performed 24–36 h later, after transfer of cells to poly-L-lysine-coated coverslip chips. Cells were maintained in Dulbecco's modified Eagle's medium (DMEM; Invitrogen) supplemented with 10% fetal calf serum and 0.2% penicillin–streptomycin.

Electrophysiology and analysis

For whole-cell voltage-clamp recording a HEKA EPC-9 amplifier with Pulse software (HEKA Elektronik, Lambrecht, Germany), and series resistance compensation of ~80%, was used. Igor software (Wavemetrics, Inc, Lake Oswego, OR, USA) was used for data analysis. Pipette resistance was 1.5–2.5 MΩ. Series resistance was < 10 MΩ. A lower series resistance (< 4 MΩ) and a waiting time of at least 5 min before oxo-M exposure was used for experiments requiring diffusion of substances from the pipette or to allow current rundown to stabilize. The exchange time for bath perfusion was about 3 s, after a delay of about 6 s. Test-pulse currents, taken every 4 s from a holding potential of −30 mV and preceded by a 2 s prepulse to +30 mV to activate the current, were analysed for mean outward current at −30 mV and maximum inward current at –100 mV. We chose cells in which erg current was 0.2–4.5 nA at −30 mV. Although there was negligible endogenous current at these potentials, we defined erg current as the current sensitive to the erg channel blocker E-4031 except in 10–15% of the cases where the seal broke before we could perform this control. We did not analyse cells giving < 0.5 nA of current unless we had the E-4031 control. No leak subtraction was used.

We corrected for current rundown in all the analysis as follows: the initial part of each record, before application of oxo-M, was fitted with a single decaying exponential curve. We then assumed that the extrapolation of this

fitted function represented the value that the control would have had at each time point if oxo-M had not been applied. Percentage inhibition by oxo-M was calculated from the greatest current reduction at −30 mV after oxo-M addition or if there was no clear reduction, the value was taken approximately 1 min after the beginning of drug application. The histograms and text give 'rundown corrected' percentage inhibition, except once where stated. In most figures, the plots of test-pulse currents *versus* time show measurements not corrected for rundown; however, the normalized plots of Fig. 9*C* and *E* are corrected. The correction was calculated by dividing the original data by the fitted rundown function described above. The resulting values were then normalized to a scale of zero (maximum inhibition) to one (starting value).

Statistics

Data values given in the text and in figures with error bars represent mean ± S.E.M. In the histograms, the number of cells used is shown on each bar in parentheses. The Hill coefficient in Fig. 1 is given as the fitted parameter ± the standard deviation of the fit. Student's unpaired *t* test (2-tailed), or, when indicated, a one-way ANOVA with a Bonferroni *post hoc* test for multiple comparisons, was used to test for significance of drug effects against controls. Student's paired *t* test (2-tailed) was used to test changes of biophysical parameters after oxo-M treatment. For the time constants of deactivation and recovery from inactivation, we also used polynomial regression analysis with three terms and confidence intervals at the 95% confidence level to fit the individual data points for control or for oxo-M conditions.

Solutions and reagents

Bath solution contained (mM) 160 NaCl, 5 KCl, 2 $CaCl_2$, 1 $MgCl_2$, 10 Hepes and 8 glucose, pH 7.4, unless otherwise indicated. Concentrations of oxo-M and E-4031 were 10 μM. Antibody to PIP_2 (Assay Designs, Ann Arbor, MI, USA) was diluted 1 : 100. Standard pipette solution contained (mM) 175 KCl, 5 $MgCl_2$, 5 Hepes, 0.1 BAPTA, 3 Na_2ATP and 0.1 Na_3GTP, at pH 7.4, unless otherwise indicated. Addition of 20 mM BAPTA to the pipette solution was counter-balanced by lowering KCl to 110 mM. The $MgCl_2$ was reduced to 1 mM in some experiments with PIP_2. Free Ca^{2+} concentrations were calculated using winMAXC (http://www.stanford.edu/~cpatton/maxc.html), assuming a Ca^{2+} contamination of 10 μM in distilled water. Chemicals were purchased from Sigma-Aldrich (St Louis, MO, USA), except E-4031 (Wako Chemicals, Richmond, VA, USA), bisindolylmaleimide V, dephostatin, calmodulin inhibitory peptide (Calbiochem, San Diego, CA, USA), and dioctanoyl PI(4,5) bisphosphate (diC_8-PIP_2, Echelon Research Laboratories, Salt Lake City, UT, USA). Stock solutions of bisindolylmaleimide I and V, calphostin C, staurosporine, phorbol 12-myristate 13-acetate (PMA), 4α-phorbol 12-myristate 13-acetate (4αPMA), and genistein in DMSO were diluted to a maximal concentration of 0.1% DMSO, a concentration at which no effect on erg current was noted. Wortmannin was diluted to a maximal concentration of 0.16% in DMSO, with no difference seen between 0.3 and 0.16% DMSO in the experiments with low concentrations of wortmannin.

Confocal imaging

tsA cells were imaged 24–48 h after transfection with the PKC-C1-EGFP optical probe and M_1 receptors. PMA or 4αPMA (500 nM) were added to the bath solution (as above except for 2.5 mM KCl). Solution exchange was by a gravity perfusion system. Images were taken every 5 s using a Leica TCS SP/MP confocal microscope and processed using Igor and Metamorph (Universal Imaging Corp., Downingtown, PA, USA).

Results

Muscarinic modulation of erg current

Depolarizing and hyperpolarizing voltage steps elicited voltage-sensitive currents in tsA cells transfected with erg1 (Fig. 1*A*). In cells not treated with other reagents, the current gradually ran down, falling on average by 1.3% per minute 5 min after breakthrough ($n = 49$). In cells also cotransfected with the M_1R, the muscarinic agonist oxo-M reduced the erg current with a slow time course (Fig. 1*A* and *B*). Inhibition of outward current at −30 mV was 30.6 ± 1.5% after correction for rundown (Fig. 1*F*, $n = 49$) and 31.9 ± 1.6% without correction. The inward current was similarly inhibited. The time constant of inhibition (τ_{inh}), determined by fitting current amplitude at −30 mV over time with a single-exponential function, averaged 18 s and ranged from 6 to 36 s. The extent of inhibition was similar for 24 s up to several-minute applications of oxo-M. Recovery was small and variable. At the end of the experiment, the specific erg blocker, E-4031, blocked almost all the remaining current (Fig. 1*B*), demonstrating a lack of outward currents endogenous to tsA cells at the voltages of the test-pulse protocol (Fig. 1*A*). (tsA cells have a relatively small endogenous outward current that just begins to activate at −20 mV and is not affected by oxo-M.) The response to oxo-M was graded, with a half-maximal inhibitory concentration of ~230 nM (Fig. 1*C*). As shown in Fig. 1*D* and *F*, activation of another G_q-coupled muscarinic receptor, the M_3 receptor, also suppressed erg current to a similar extent (~30%). Little apparent inhibition was seen in the absence of M_1 receptor expression (Fig. 1*E* and *F*) or in the presence of the muscarinic receptor antagonist atropine (Fig. 1*F*). In all

subsequent experiments, the cells were transfected with the M_1R.

Oxo-M reduces maximal current and slightly shifts activation of erg

The experiments in Fig. 2 measured the activation of erg current. After a step from the holding potential of −80 mV to progressively more depolarized potentials, the steady-state current initially increased (slowly rising traces in Fig. 2*A*) and then began to decrease at higher potentials (faster rising traces). This biphasic pattern results from the interplay of voltage-dependent activation and inactivation. Since inactivation is quickly removed at negative potentials, we measured activation gating by analysing the peak inward tail-current amplitude at −100 mV after a depolarizing test pulse. Application of oxo-M caused a small but significant positive shift of the midpoint of activation of about 5 mV, from -8.3 ± 3.2 mV in control conditions to -3.5 ± 3.5 mV after oxo-M ($P \leq 0.003$, $n = 7$; Fig. 2*B*). The slope factor did not change significantly. The maximum tail-current amplitude determined by fitted curve in Fig. 2*B* was reduced 33% ($P \leq 0.001$) by oxo-M treatment. To check that these changes were not simply a consequence of whole-cell dialysis over time, we performed control experiments with two successive activation protocols separated by a similar interval (2–3 min). There was no significant shift in the midpoint of activation (first -6.2 ± 3.6 mV, second -3.8 ± 4.3 mV, shift of 2.3 ± 1.7 mV, not significant).

We also tested for a change in the time dependence of activation by using an envelope-of-tails protocol.

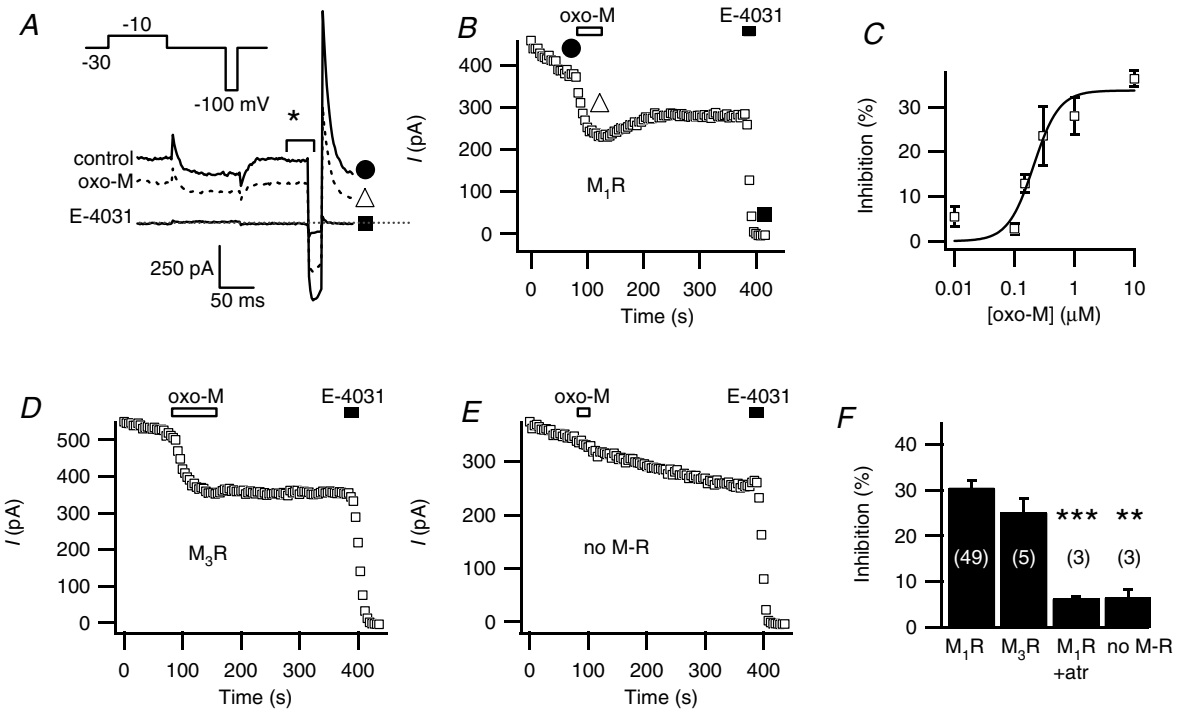

Figure 1. M_1- and M_3-muscarinic receptors inhibit erg current
A, representative current traces from a cell expressing the M_1 muscarinic receptor (M_1R) and erg. Test pulses were given every 4 s from a holding potential of −30 mV. The voltage protocol (inset) is preceded by a prepulse to +30 mV for 2 s. The three current traces correspond to the marked points in *B*: before oxo-M (●), during application of the agonist oxo-M (Δ) and after application of the blocker E-4031 (■). *B*, mean outward current at –30 mV (in the period marked * in *A*) is plotted *versus* time. The graph starts 1 min before oxo-M application. Bars indicate application of oxo-M (10 μM) and E-4031 (10 μM). The initial few minutes after achieving whole cell have been omitted. *C*, dose–response relation for oxo-M suppression of erg ($n = 3$–4 for each concentration). A Hill equation fitted to all data points gave half-maximal inhibition at 230 nM and a Hill coefficient of 2.5 ± 1.2 (standard deviation of fit). *D,* muscarinic suppression of erg in a cell transfected with the M_3 muscarinic receptor (M_3R) using the same pulse protocol as in *A*. *E*, lack of action of oxo-M in a cell not transfected with a muscarinic receptor (squares). *F*, erg current inhibition after oxo-M application in cells transfected with M_1R, M_3R, M_1R after 4 min exposure to 10 μM atropine (M_1R + atr), or no muscarinic receptor (no M-R). $^{**}P = 0.005$ and $^{***}P = 0.0005$ indicate statistical significance *versus* controls.

Figure 2*C* shows the pulse protocol and representative control currents. Although the mean time constant of activation appeared to lengthen (247 ± 92 ms, control *versus* 522 ± 45 ms, oxo-M), the difference did not reach statistical significance ($n = 5$, Fig. 2*D*). Even if real, such a change in time course should not significantly affect the outward current measured with a test pulse following the 2 s depolarizing prepulse we usually used to activate erg channels. In conclusion, oxo-M reduces erg current both by a reduction in maximum current as well as by a small positive shift of the voltage dependence of activation.

A small shift in the voltage dependence of erg availability

As anticipated from the experiments on activation, oxo-M also shifted the voltage dependence of deactivation to more positive potentials and the effect was small. The currents and protocol used to isolate isochronal erg deactivation are shown in Fig. 3*A* and *B*. A −20 mV holding potential served to minimize erg deactivation, and channels were then fully activated by an initial depolarization to +30 mV for 2 s preceding each prepulse. After a subsequent long pulse at different potentials to achieve deactivation, the tail current amplitude at −100 mV was measured and plotted against the prepulse potential (Fig. 3*C*). Application of oxo-M reduced the overall current amplitude and shifted the midpoint of deactivation 8.0 ± 1.3 mV (from -44 ± 5 mV to -36 ± 6 mV, $P \leq 0.01$, $n = 4$), similar to the shift found for activation. To determine whether oxo-M changed the time course of deactivation, we examined deactivation with test pulses ranging from −100 mV to −40 mV. The current transient was fitted with the sum of three exponentials, corresponding to the time constants for quick recovery from inactivation (τ_{rec}, discussed in the next paragraph) and for the fast and a slow components of deactivation (τ_{fast}, τ_{slow}, Fig. 3*D* and *E*). At most potentials, there was a trend for deactivation in individual experiments to be speeded by oxo-M, but the change reached significance only at a few potentials. There was an overlap of the confidence interval of a polynomial regression at all potentials (not shown). The inset in Fig. 3*A* illustrates the near overlap of current decay at −70 mV before and after oxo-M treatment.

Minor effects on inactivation

Inactivation was measured with the two-step protocol of Fig. 4*A*. Cells with fully activated channels were held briefly at −100 mV to relieve inactivation, and then stepped to various potentials to allow inactivation to redevelop (Fig. 4*A*). Steady-state inactivation was calculated as the

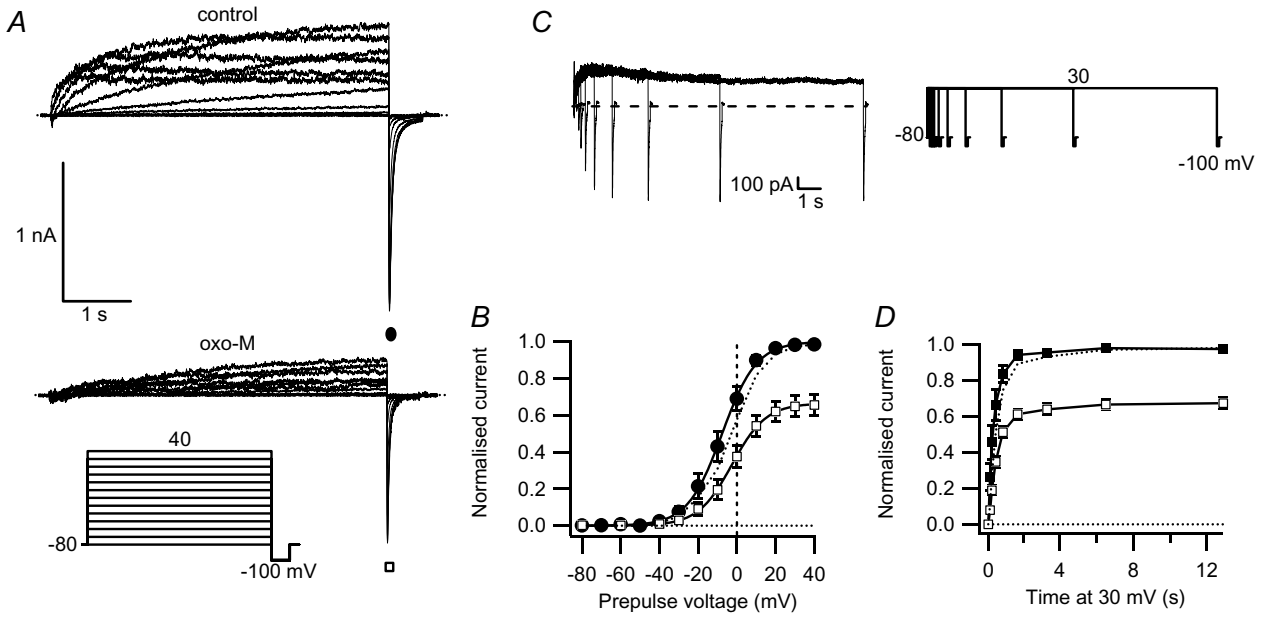

Figure 2. M_1R stimulation reduces maximal erg current activation
A, erg currents elicited by the activation protocol (inset) before and during 10 μM oxo-M. *B,* maximal tail current amplitudes, taken at −100 mV after stepping to different voltages for 5 s, for control (●) and after treatment with oxo-M (□, $n = 7$). Values normalized to maximal current under control conditions are plotted against the prepulse potential. The dotted curve shows the current after oxo-M scaled to the control current amplitude. *C*, tail-current pulse protocol and representative current traces for the time dependence of activation. *D*, time course of activation, with normalized tail current shown at different times, for control (■), after oxo-M (□), and after oxo-M scaled to control (dotted line).

steady-state current after inactivation at each potential divided by the initial current before inactivation. At negative potentials, deactivation became rapid enough to contribute slightly to current reduction, therefore potentials more negative than −60 mV were not studied. The voltage dependence of steady-state inactivation was not changed by oxo-M (Fig. 4*B*). The voltage-dependent time constant of *development* of inactivation (τ_{inact}), fitted as a single exponential to the current decay, was also not significantly changed (Fig. 4*C*). Finally, the time constants for *recovery* from inactivation (τ_{rec}), measured from deactivation protocols as described in the last section, showed a small statistically significant decrease with oxo-M at the more depolarized potentials (Fig. 4*D*), but the confidence interval of a polynomial regression overlapped at all potentials (not shown).

G proteins involved in muscarinic inhibition of erg current

Which G protein(s) mediate the muscarinic signal? The modulation was not changed by prior bath application of 50 μM *N*-ethylmaleimide (NEM; Fig. 5*A*, $n = 3$), which would completely block the $G_{i/o}$-dependent inhibition of N-type Ca^{2+} channels by somatostatin (Shapiro *et al.* 1994). Coexpression of a constitutively active form of G_q

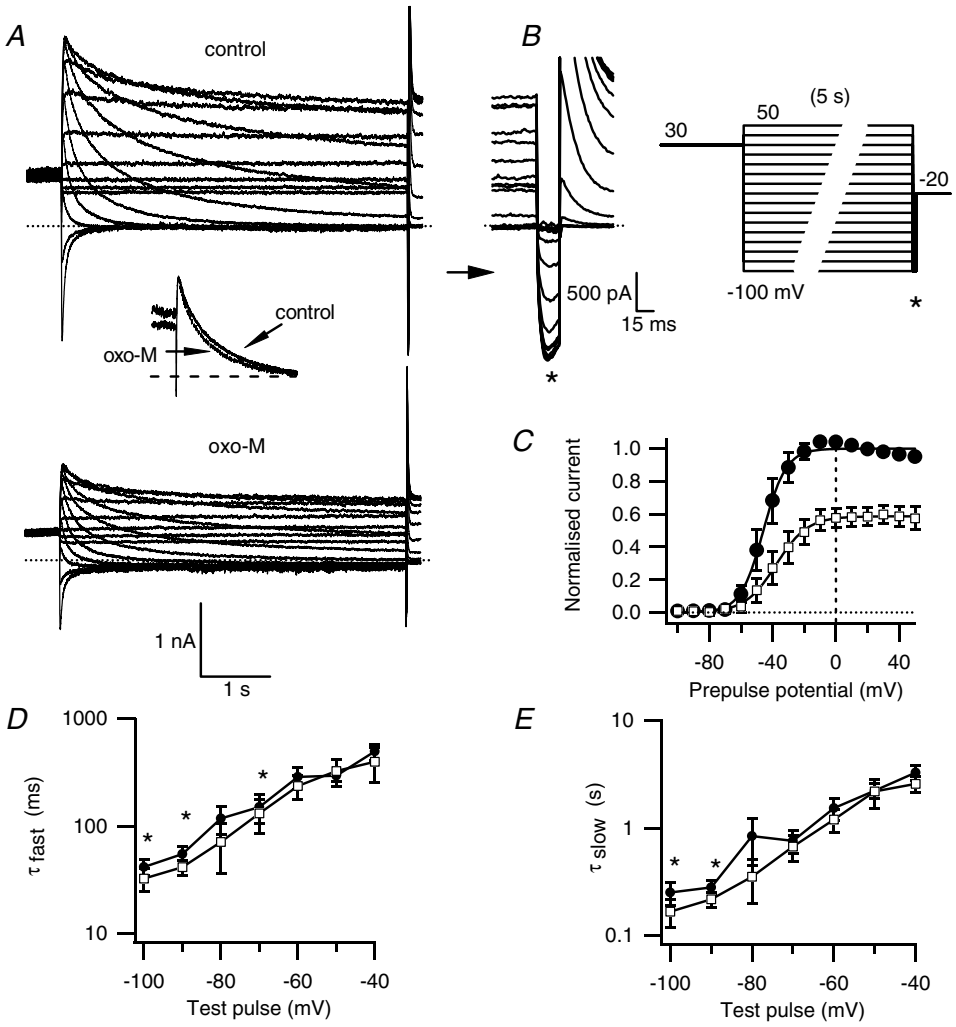

Figure 3. Muscarinic inhibition produces only minor changes in deactivation
A, erg current traces before and after oxo-M application, using the deactivation protocol in *B*. Inset of *A* shows an overlay of the prepulse current decay at −70 mV before and after oxo-M (scaled to control). The maximal tail current amplitudes at −100 mV (* on sweep-magnified traces and protocol), are measured after a 5 s prepulse that allows deactivation at different prepulse potentials. *C*, tail current amplitudes for control (●) or oxo-M (□) conditions normalized to maximal current ($n = 4$) and plotted against prepulse potential. *D* and *E*, fast (τ_{fast}) and slow (τ_{slow}) time constants of deactivation and a time constant for recovery from inactivation (see Fig. 4) were calculated by a triple exponential fit of the current deactivation at the prepulse potential for control (●) or oxo-M (□) ($n = 4$, * $P \leq 0.05$). The holding potential was −20 mV to minimize deactivation between test pulses. To maximize current activation, a 2 s prepulse to +30 mV preceded each test sweep. All current traces are E-4031-sensitive currents.

(Fig. 5*B*) completely abolished erg current, while leaving the small endogenous outward current intact (7/8 cells). In control cells transfected with constitutively active α-subunits of G_s and G_{13}, erg current was still present, although reduced compared to controls (or to cells transfected with the same amount of RGS2 cDNA; Fig. 5*B*). Inhibition of erg by oxo-M is attenuated when the $G_{q/11}$ pathway is blocked with dominant-negative G_q (Fig. 5*C* and *E*, $P \leq 0.0001$, $n = 6$). Unfortunately we could not test the role of the G_q effector PLC directly, because the PLC inhibitor U73122 and its inactive analogue U73343 totally abolished erg current. Expression of dominant-negative G_{13}, did not attenuate responses (Fig. 5*F*). Coexpression of the regulator of G protein signalling RGS2 attenuated erg modulation by oxo-M in 10 out of 13 cells, leaving a mean inhibition of $15.8 \pm 3.2\%$ ($P \leq 0.01$, $n = 13$; Fig. 5*C* and *D*). RGS2 binds specifically to activated G_q and prevents interaction with effectors (Heximer *et al.* 1997; Bernstein *et al.* 2004). For example, RGS2 blocks the slow M_1-muscarinic inhibition of N-type Ca^{2+} channels in HEK293 cells (Melliti *et al.* 2001). Thus, we obtained multiple lines of evidence that G_q mediates muscarinic suppression of erg.

Cytoplasmic calcium is required but not a calcium signal

As shown in Fig. 6*A* and *B*, modulation by oxo-M is sensitive to chelating intracellular Ca^{2+} to very low levels. Adding 20 mM BAPTA in the pipette (< 1 nM calculated free Ca^{2+}) attenuated muscarinic suppression in 9 out of 11 cells ($19 \pm 4\%$, $n = 9$, with BAPTA, *versus* $43 \pm 5\%$, $n = 5$ for controls from the same day, $P \leq 0.01$, Fig. 6*D*). The time course of inhibition was also significantly slowed as summarized in Fig. 6*E*.

Does the sensitivity to cytoplasmic Ca^{2+} imply that a Ca^{2+} *signal* is essential in the muscarinic modulation of erg? We followed a strategy we had used before of clamping intracellular Ca^{2+} to a typical resting level with a strong BAPTA buffer (Beech *et al.* 1991) and simultaneously blocking several sources of Ca^{2+} flux into the cytoplasm (Shapiro *et al.* 2000). The pipette solution included 20 mM BAPTA and 10 mM Ca^{2+} (to buffer at 129 nM calculated free Ca^{2+}) and also the IP_3 receptor blocker pentosan polysulphate (PPS, 50 μg ml^{-1}). Intracellular Ca^{2+} stores were depleted with the Ca^{2+}-ATPase blocker thapsigargin (2 μM, > 20 min pretreatment), and extracellular Ca^{2+} was removed. We have previously shown that these conditions block M_1 receptor-induced Ca^{2+} transients in the same cell type (Shapiro *et al.* 2000). With this panel of Ca^{2+}-stabilizing agents ('buffered calcium'), muscarinic suppression remained normal in amplitude, although possibly slowed in time course (Fig. 6*C*, *D* and *E*). We conclude that a Ca^{2+} transient is not essential for M_1 muscarinic receptor suppression of erg. Evidently, as seen with M-current (Beech *et al.* 1991; Shapiro *et al.* 2000), Ca^{2+} plays a permissive role for muscarinic suppression of erg, but is not a necessary signal.

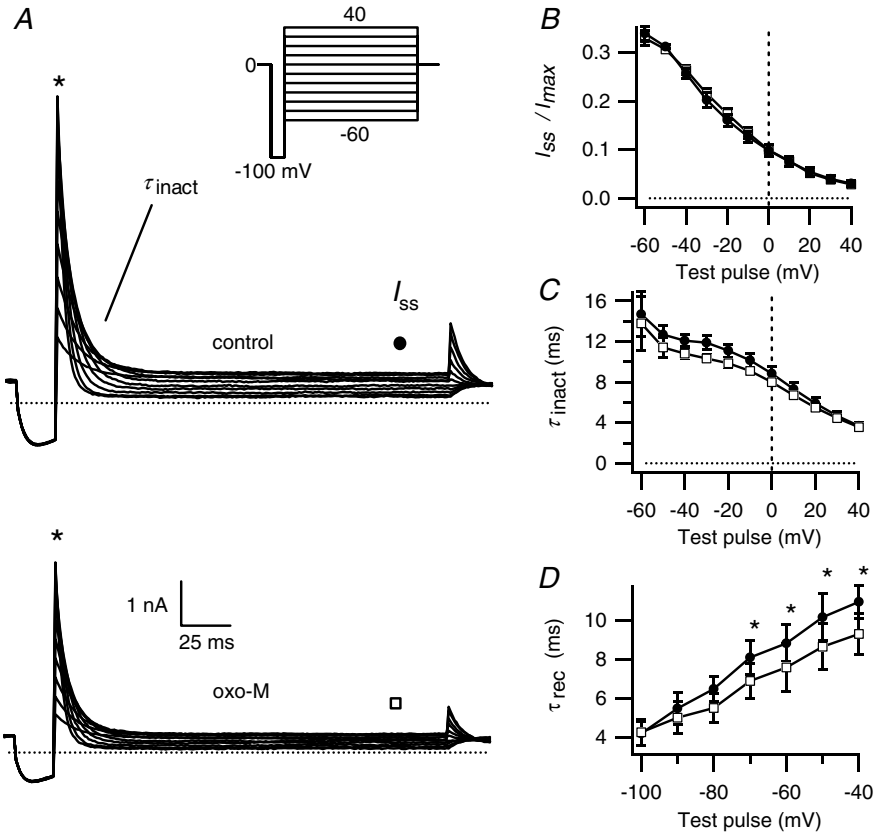

Figure 4. Muscarinic stimulation has only a minor effect on inactivation
A, erg current traces before and after oxo-M application using the inactivation protocol shown in the inset. An additional prepulse to +30 mV for 2 s from the holding potential of 0 mV is not depicted. *B*, voltage dependence of steady-state inactivation as seen in the test pulse plotted as the ratio of steady-state current I_{ss} at (●) for control or at (□) for oxo-M, divided by the peak current I_{max} at *, as depicted in *A*. *C*, time constant of inactivation (τ_{inact}), for control (●) and oxo-M (□). *D*, time constant of recovery from inactivation (τ_{rec}), taken from a fit of the deactivation protocol as described in Fig. 3, for control (●) and oxo-M (□) ($n = 4$, * $P \leq 0.05$). All currents are E-4031-sensitive.

Another EAG family member, hEAG1, is modulated by Ca^{2+}–calmodulin (Schönherr *et al.* 2000). We followed an approach used successfully to demonstrate calmodulin dependence of bradykinin receptor action (but not M_1 receptor action) in the suppression of M-current (Gamper & Shapiro, 2003). We compared cells coexpressing a wild-type (wtCaM) construct with cells coexpressing a dominant-negative (dnCaM) form of calmodulin. The dnCaM has an alanine substitution in each of the four Ca^{2+}-binding EF hands (D20A, D56A, D93A, D129A), which destroys the ability to bind Ca^{2+} (Geiser *et al.* 1991). The two sets of cells responded equally to oxo-M (wtCaM: $20 \pm 3\%$, $n = 3$; dnCaM: $22 \pm 3\%$, $n = 4$).

Kinases are not required for development of muscarinic inhibition of erg

Muscarinic receptors and G_q can activate several protein kinase pathways, notably protein kinase C (PKC), but other kinases as well (Lanzafame *et al.* 2003). We tested the need for kinase activity for the development of muscarinic inhibition by using a panel of kinase inhibitors and stimulators. We first tested the PKC-specific inhibitor bisindolylmaleimide I (1 μM in the bath and preincubation for > 20 min) and the broad kinase inhibitor staurosporine (1 μM in the bath and pipette). We chose inhibitor concentrations that were more than enough to block phorbol ester-stimulated actions on Ca^{2+} channels and receptors in our previous experiments on rat neurones and the corticotrope AtT-20 cells (Shapiro *et al.* 1996; Garcia *et al.* 1998). While greatly accelerating rundown of current (e.g. Fig. 7*A*), the two kinase inhibitors did not alter (rundown-corrected) inhibition of erg current by 10 μM oxo-M (Fig. 7*D*). Remarkably the inhibition by 1 μM oxo-M even seemed to be enhanced. The inactive analogue bisindolylmaleimide V did not have this effect. Surprisingly, calphostin C (1 μM), which inhibits PKC at its DAG-binding site rather than at the ATP-binding site like the other two inhibitors, significantly attenuated the oxo-M inhibition of erg (Fig. 7*B* and *D*). Nevertheless, applying the active phorbol ester PMA (500 nM, $n = 8$) did not attenuate oxo-M inhibition of erg more than the inactive homologue 4αPMA ($n = 4$) did (Fig. 7*D*). In contrast to previous results in *Xenopus* oocytes and GH_3/B_6 cells (Barros *et al.* 1998; Schledermann *et al.* 2001), in our cell system PMA caused no shift in the midpoint of activation (0.0 ± 0.5 mV), although subsequent oxo-M still caused a small shift ($+8.1 \pm 1.7$ mV, $P \leq 0.05$, $n = 3$). As a control, we confirmed the activity of the PMA solution using the confocal microscope by monitoring the translocation of the diacylglycerol binding domain of PKC fused to the enhanced green fluorescent protein

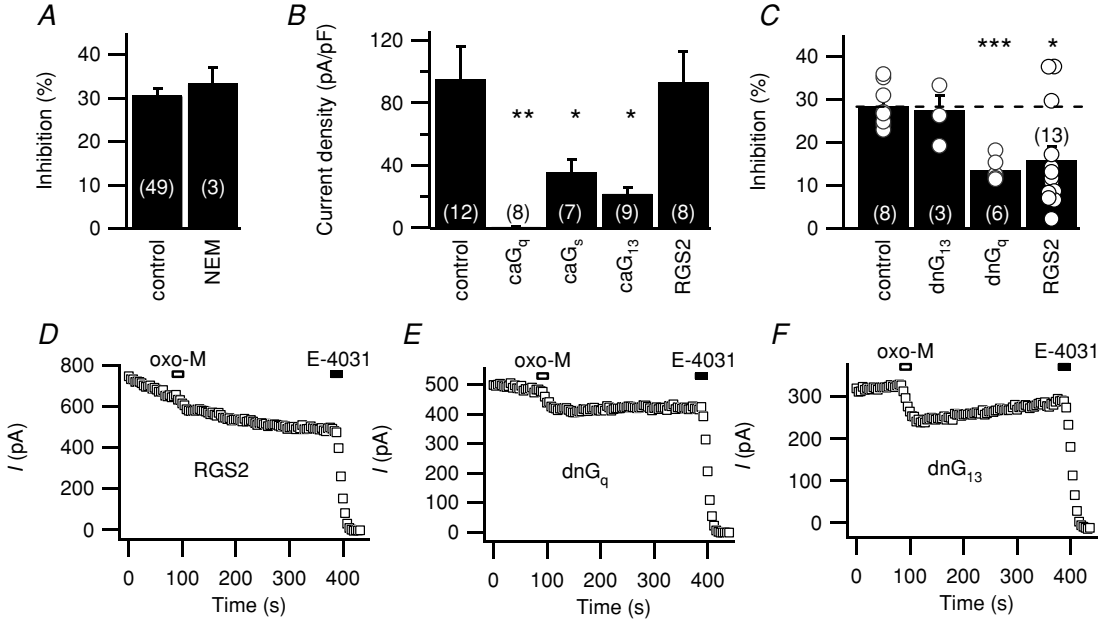

Figure 5. G protein involvement in muscarinic suppression of erg
A, muscarinic suppression of current in control cells and cells preincubated with the $G_{i/o}$ inhibitor *N*-ethylmaleimide (NEM; 50 μM) for 2 min. The test pulse protocol for this and subsequent experiments is as in Fig. 1. *B*, initial density of current in cells overexpressing constitutively active forms of G_q, G_s or G_{13} (caG_q, caG_s or caG_{13}) or RGS2. * $P \leq 0.05$ and ** $P \leq 0.005$ indicate significant difference from controls. *C*, percentage suppression in cells overexpressing dominant-negative G_{13} or G_q (dnG_{13}, dnG_q), or RGS2. Individual observations are shown as open circles. * $P \leq 0.05$ and *** $P \leq 0.0005$ indicate significant difference from controls. *D*, *E* and *F*, representative time courses of test currents during inhibition by oxo-M in cells cotransfected with the indicated genes. For RGS2, the example is representative of 10/13 cells.

(PKC-C1-EGFP probe). As expected, this DAG probe moved from a uniform cytoplasmic distribution to the plasma membrane upon application of PMA but not of inactive 4αPMA (Fig. 7*E*).

A general block of protein kinase and lipid kinase reactions can be achieved by removing all hydrolysable ATP. Replacing the 3 mM ATP in the pipette with 4 mM of non-hydrolysable AMP-PCP ($n = 4$) did not prevent inhibition of erg by oxo-M (Fig. 7*C* and *D*). As with staurosporine or bisindolylmaleimide I, rundown of current was very rapid with AMP-PCP.

Recent studies suggest that erg current can be modulated by tyrosine kinases and phosphatases (Cayabyab & Schlichter, 2002; Cayabyab *et al.* 2002). As shown in Fig. 7*D*, substances that block kinases or phosphatases did not significantly prevent muscarinic suppression of erg. Neither the tyrosine kinase inhibitor genistein (50 μM, $n = 4$) nor the tyrosine phosphatase inhibitor dephostatin (50 μM, $n = 4$) prevented inhibition of erg current by oxo-M. Genistein itself strongly reduced the current by about 60% over the initial 5 min as in previous studies (Schledermann *et al.* 2001; Cayabyab & Schlichter, 2002). The reduction was partially reversed by removal of genistein. Dephostatin (50 μM) also caused a slow reduction of the current (5 min application, $n = 4$). The general phosphatase inhibitor orthovanadate did not prevent inhibition when included in the pipette (0.5 mM, $n = 4$).

We tested the protein- and lipid-kinase inhibitor wortmannin. A 30 μM concentration did not prevent oxo-M inhibition of erg (Fig. 7*D*). This concentration suffices to block myosin light chain kinase, PI 3-kinase, and PI 4-kinase (see Suh & Hille, 2002).

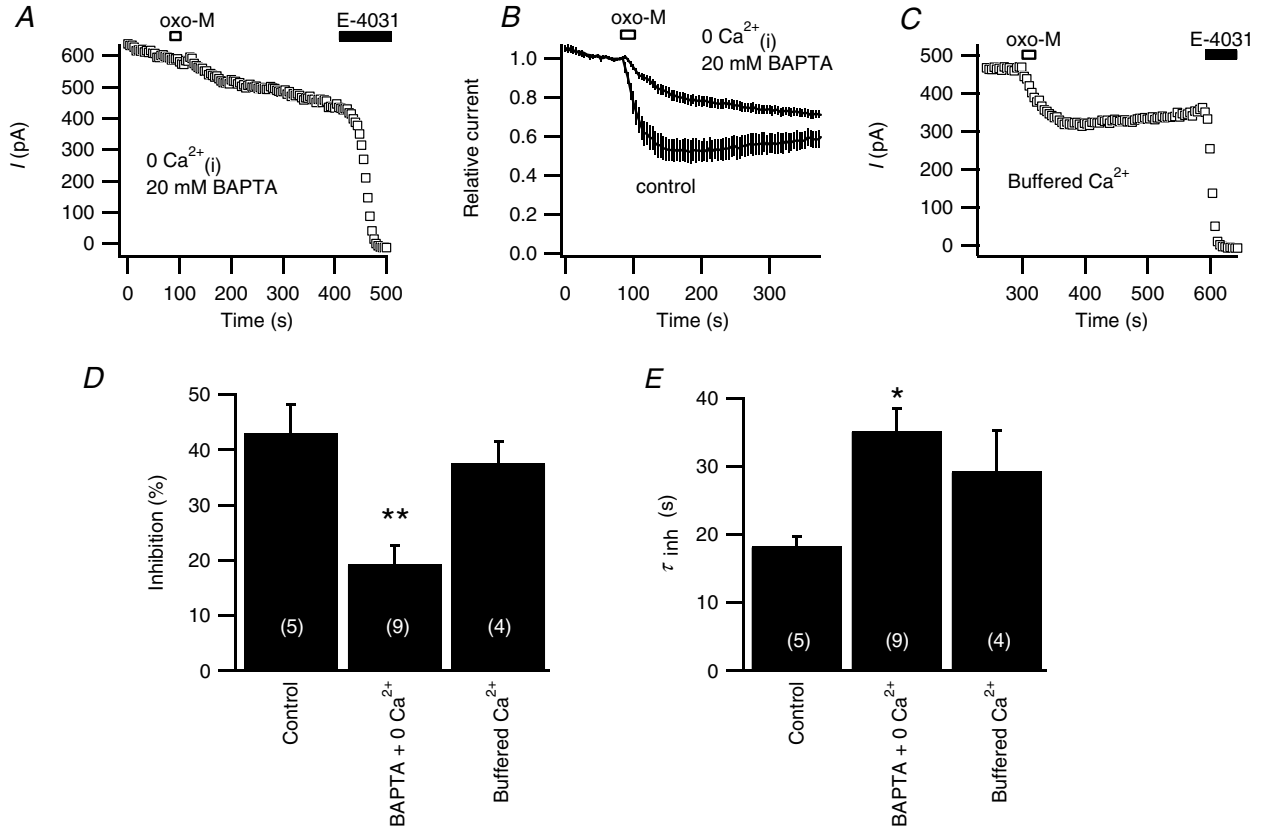

Figure 6. Full muscarinic modulation of erg requires a minimum amount of Ca^{2+}
A, representative response to oxo-M when the internal Ca^{2+} was clamped to very low levels by a high concentration of BAPTA (20 mM) in the pipette and no Ca^{2+} was included in the pipette solution. *B*, averaged time course of oxo-M action using the same protocol as in *A* ($n = 9$), compared with controls from the same experimental days ($n = 5$). *C*, representative experiment with 'buffered Ca^{2+}' comprising: internal Ca^{2+} clamped at 129 nM with 20 mM BAPTA + 10 mM Ca^{2+} + 50 μg ml^{-1} pentosan polysulphate (PPS) in the pipette, no Ca^{2+} in the bath, and 2 μM thapsigargin preincubation for > 20 min. *D* and *E*, amplitudes and time constants (τ_{inh}) of exponential fits of oxo-M inhibition in control cells, in cells with internal free Ca^{2+} buffered to less than 1 nM with 20 mM BAPTA and no Ca^{2+} added to the pipette solution (BAPTA + 0 Ca^{2+}), and or in cells with 'buffered Ca^{2+}' (* $P \leq 0.05$, ** $P \leq 0.01$, *versus* controls from the same day, ANOVA).

The Rho signalling pathway is reported to inhibit erg current upon activation of the thyrotropin-releasing hormone (TRH) receptor (Storey *et al.* 2002). RhoA/B/C can be inhibited by C3 toxin, the ADP-ribosyltransferase C3 of *Clostridium botulinum*, in the presence of NADPH (Lang *et al.* 1992; Just *et al.* 2001). However, we found no alteration of oxo-M inhibition of erg current when the pipette solution contained C3 toxin (3 μg ml^{-1}) and NADPH (1 mM, Fig. 7*D*).

Is there a role for PIP_2 in recovery from muscarinic inhibition?

The phospholipid PIP_2 is essential for the activity of many membrane channels and transporters (Hilgemann *et al.* 2001). In our tsA cells, stimulation of M_1 receptors activates PLC (Suh *et al.* 2004), which by depleting PIP_2 decreases the activity of ion channels such as the KCNQ2/3 channel (Suh & Hille, 2002). Then recovery after inhibition requires resynthesis of PIP_2 by lipid kinases (Suh & Hille, 2002) or exogenous delivery of PIP_2 (Zhang *et al.* 2003). We hoped to test this concept for erg channels.

We began by looking at the direct effect of adding the short-chain, soluble dioctanoyl-PIP_2 (diC_8-PIP_2) to the whole-cell pipette solution. Including 8 or 100 μM diC_8-PIP_2 in the recording pipette (with only 3 or 1 mM Mg^{2+}, respectively, to minimize micelle formation) produced no significant change in the oxo-M inhibition of erg compared to control cells (Fig. 8*A*, *C* and *D*). An 8 μM concentration sufficed in published work to

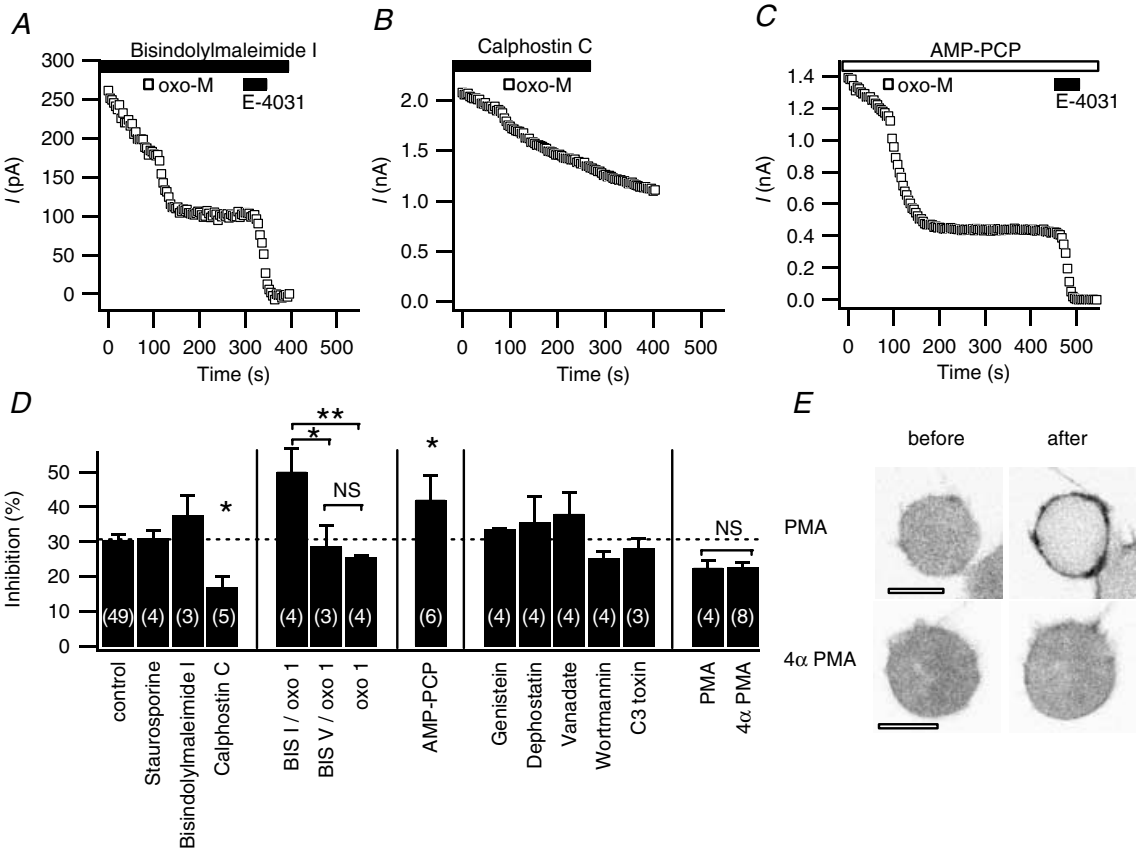

Figure 7. Kinases are not involved in erg current inhibition by oxo-M
A, *B* and *C*, erg current inhibition by oxo-M after pretreatment with bisindolylmaleimide I (1 μM in the bath, following preincubation for 20–50 min), calphostin C (1 μM in the bath), and AMP-PCP (4 mM in the pipette, no ATP). Application in the bath is indicated by filled bars and application in the pipette solution by open bars. *D*, amplitude of muscarinic inhibition under control conditions and after applying one of the following: staurosporine, bisindolylmaleimide I, bisindolylmaleimide V, or calphostin C (1 μM); AMP-PCP replacing all ATP in the pipette (4 mM AMP-PCP); genistein (50 μM); dephostatin (50 μM); orthovanadate (0.5 mM); wortmannin (30 μM); or C3 toxin (3 μg ml^{-1} in the pipette solution with 1 mM NADPH); phorbol 12-myristate 13-acetate (PMA; 500 nM); or 4αPMA (500 nM). In one group of experiments, 1 μM oxo-M was used as indicated (oxo 1) instead of 10 μM oxo-M, and compared to same-day controls. Application of oxo-M was > 5 min after achieving whole-cell configuration to allow for diffusion of substances from the pipette. Inhibitors were applied in the bath for > 5 min prior to oxo-M, except for PMA (2 min) and bisindolylmaleimide I and V (additional > 20 min pre-incubation). NS, not significant, * $P \leq 0.05$, ** $P \leq 0.01$. *E*, representative confocal images of cells transfected with the PKC-C1-EGFP probe and M_1R, 3 min after a 2 min treatment with either PMA ($n = 5$) or 4αPMA ($n = 4$). Images are in negative contrast so that fluorescence is black. Scale bars are 10 μm.

enhance recovery of TRPM7 channels from muscarinic inhibition (Runnels *et al.* 2002). The diC_8-PIP_2 pipette also did not enhance the poor recovery of erg current from muscarinic suppression or induce a run-up of the current. A complementary test, including PIP_2 antibody in the pipette and allowing 20 min for diffusion, did not lead to more rundown than in controls. Again inhibition of erg current by oxo-M was not significantly altered (Fig. 8*B* and *D*).

In another set of experiments, we tested the possibility that recovery from muscarinic inhibition is dependent on enzymatic resynthesis of PIP_2. The first strategy was to compare the effects of wortmannin at two concentrations. The lower concentration (1 μM) would be enough to block PI 3-kinase and myosin light-chain kinase, whereas the high concentration (50 μM) would block PI 4-kinase as well (preventing PIP_2 resynthesis). Individual traces (Fig. 9*A* and *B*) and rundown-corrected average traces (Fig. 9*C*) show significantly less recovery (Fig. 9*B* and *C*) with the higher concentration of wortmannin (summarized in Fig. 9*F*). The second approach was to deprive the cell of ATP needed for the activity of PI 4-kinase and PIP 5-kinase (and all other kinases). When AMP-PCP was included in an ATP-free pipette solution, recovery was less than in controls (Fig. 9*E* and *F*). In these experiments, we did not have a set of same-day controls with standard pipette solution; however, when compared with a grand average of all controls on other days, the effects of wortmannin and AMP-PCP did not reach statistical significance. A difficulty was that recovery was very variable among cells, and it was far from complete.

Discussion

Comparison to previous work

Our study shows that the activation of M_1 muscarinic receptors inhibits erg1 current with a slow time course

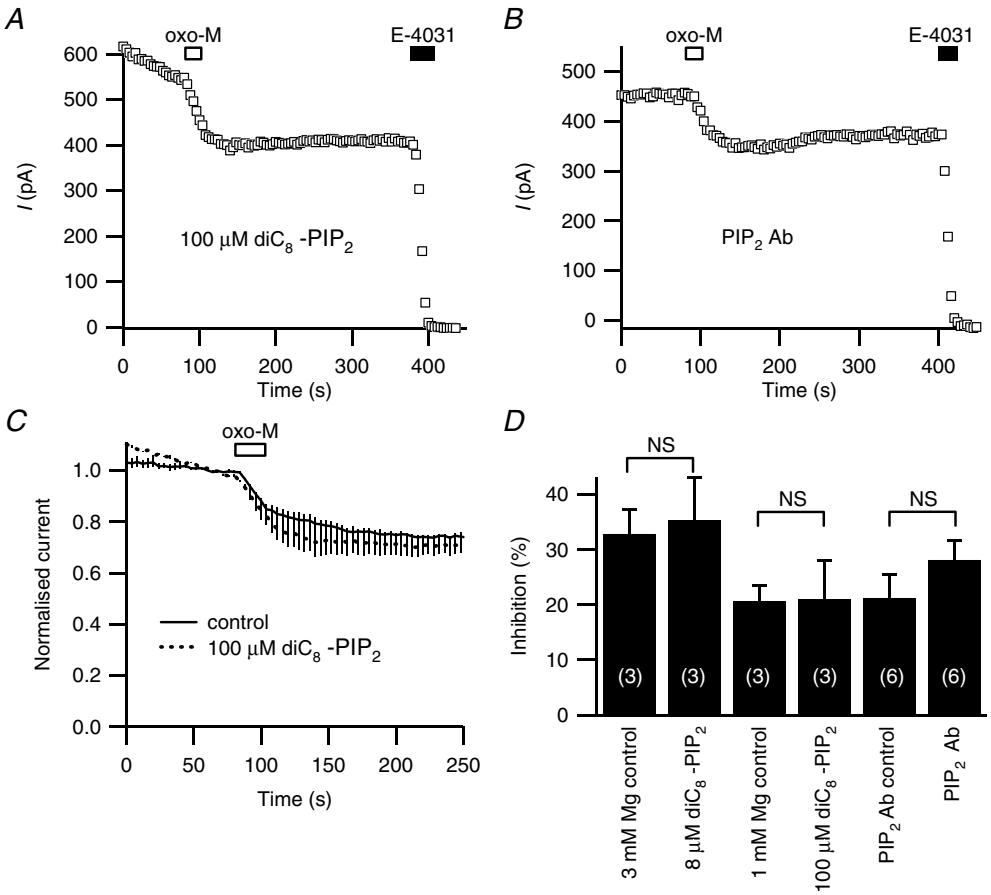

Figure 8. Tests with application and removal of PIP_2
A, representative response to oxo-M when the pipette included 100 μM dioctanoyl-PIP_2 (diC_8-PIP_2, tip filled with normal solution to facilitate seal formation, > 10 min wait to allow diffusion). *B*, representative response to oxo-M when the pipette included PIP_2 antibody for 20 min. *C*, averaged time courses of muscarinic inhibition with 100 μM diC_8-PIP_2 and controls (with 1 mM instead of 5 mM Mg^{2+}). *D*, summary of whole-cell experiments with diC_8-PIP_2 and with PIP_2 antibody (Ab).

(∼18 s) in a tsA-cell expression system. The development of inhibition is G_q dependent, Ca^{2+} dependent, and kinase and ATP independent, and a principal effect is to reduce the maximum available current. Recovery is slowed by wortmannin, and rundown is accelerated by wortmannin and ATP-free solutions. These properties are reminiscent of the slow M_1 receptor-mediated inhibition of M-current and of N-type and L-type Ca^{2+} channels in sympathetic neurones (Beech *et al.* 1991; Bernheim *et al.* 1991; Mathie *et al.* 1992; Marrion, 1997; Haley *et al.* 2000). In addition,

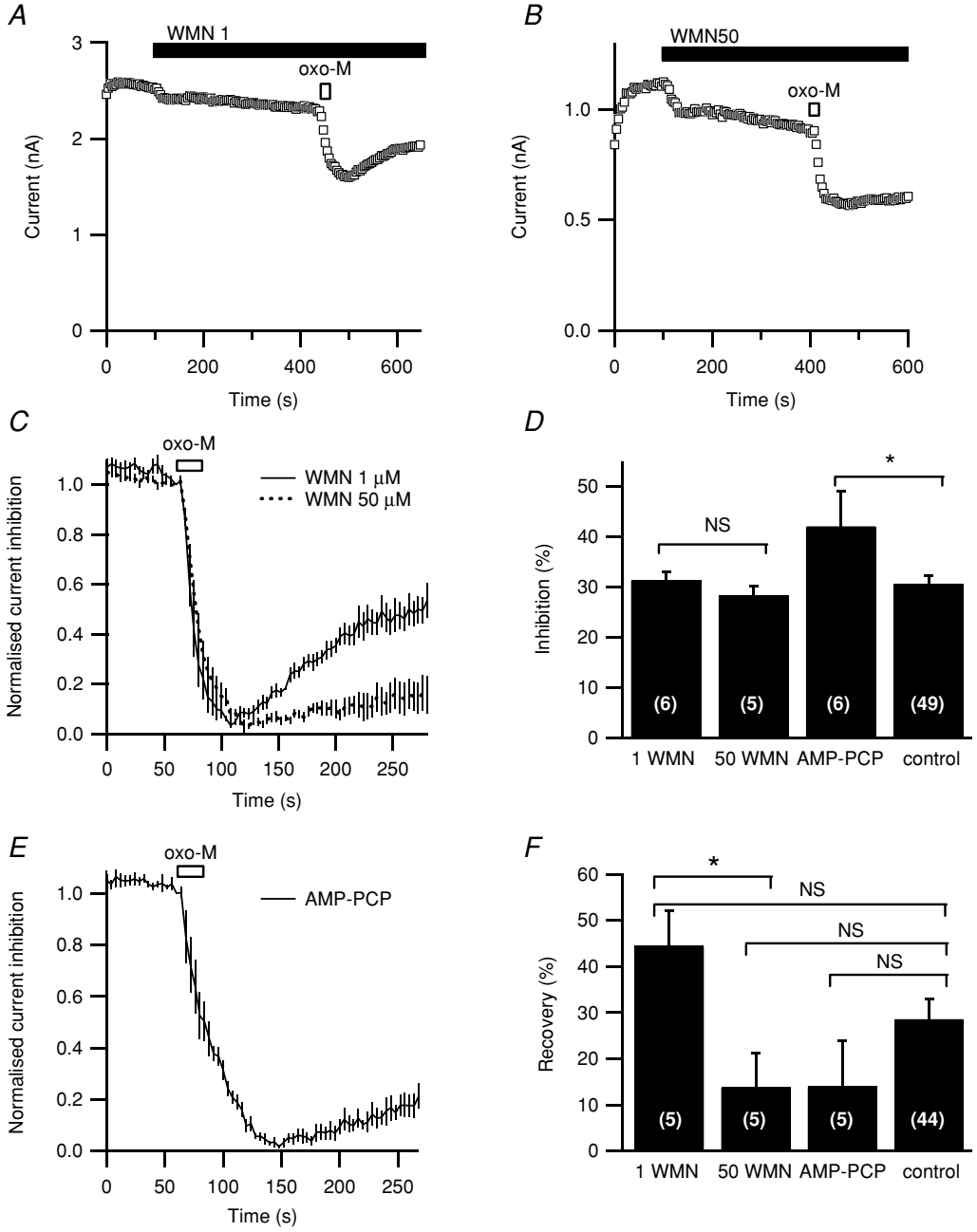

Figure 9. Effects of wortmannin and removal of ATP
A and *B*, representative responses to oxo-M after preincubating with 1 μM or 50 μM wortmannin (WMN1 and WMN50). *C*, averaged time courses of muscarinic suppression and recovery after preincubation with 1 μM or 50 μM wortmannin ($n = 5$ for each). These data have been corrected for rundown and normalized (see Methods). *D*, summary of extent of inhibition with wortmannin or with 4 mM of the non-hydrolysable AMP-PCP replacing all pipette ATP. *E*, averaged time course of muscarinic suppression and recovery from inhibition with 4 mM AMP-PCP included in the pipette instead of ATP, corrected and normalized as in *C*. *F*, recovery from muscarinic inhibition measured with correction for rundown 3 min after maximal oxo-M inhibition with wortmannin or ATP-free pipette solution. $^*P \leq 0.05$.

the muscarinic inhibition is accompanied by a small shift in the voltage dependence of activation to more positive voltages with little change of inactivation. The inhibition of erg is only partial, and recovery is weak and variable in our whole-cell recording. One prior study described M_1R-mediated inhibition of mouse erg in neuroblastoma cells and of merg1a overexpressed in Chinese hamster ovary (CHO) cells (Selyanko *et al.* 1999). Using perforated patches, they found that muscarinic inhibition was slow and involved an acceleration of the deactivation kinetics. We observed a trend toward faster deactivation associated with muscarinic inhibition, but it was less marked than the decrease in available current. A subsequent study in the same neuroblastoma cells using whole-cell patch clamp found that current rundown and muscarinic modulation of mouse erg and KCNQ current were sensitive to cyclic ADP ribose (Higashida *et al.* 2000), which may alter Ca^{2+}.

Our more in-depth analysis of M_1 receptor-mediated inhibition of erg currents is consistent with previous work showing reduction of erg currents by other phospholipase-C-coupled receptors. Most published work involves inhibition of endogenous and over-expressed erg1 by the endogenous G_q-coupled TRH receptor in clonal rat anterior pituitary cells (Bauer *et al.* 1990; Schledermann *et al.* 2001; Storey *et al.* 2002; Gómez-Varela *et al.* 2003) or inhibition of exogenous HERG by the over-expressed TRH receptor in *Xenopus* oocytes (Barros *et al.* 1998). One report shows HERG inhibition by the phospholipase-C-coupled α1A adrenergic receptor in a CHO cell expression system (Bian *et al.* 2001). All reports, including ours, find a slow reduction of currents that is due in part to positive shifts of activation and in part to a depression of the maximum current. Some previous reports describe the agonist-induced inhibition as Ca^{2+} requiring (Bauer *et al.* 1990) or as kinase independent (Schledermann *et al.* 2001; Gómez-Varela *et al.* 2003).

The initial steps

To date the principal reports of erg/HERG inhibition via G-protein-coupled receptors have used TRH, α1-adreno- and M_1 receptors. All of these receptors are known to couple to $G_{q/11}$ and thus stimulate phospholipase C. In addition, they may couple to other G proteins. We believe that signalling via $G_{q/11}$ suffices to produce inhibition of erg1 current. Expression of constitutively active G_q suppresses erg current almost completely. Expression of constitutively active G_s or G_{13} suppresses the current only partly. Muscarinic inhibition was strongly reduced by expressing RGS2 or dominant-negative G_q. Dominant-negative G_{13} did not decrease muscarinic inhibition, nor did treatments with the G_o/G_i-modifier NEM. The typical ~30% inhibition of erg current with several minutes of stimulation by oxo-M is nonetheless much weaker than that with overnight expression of constitutively active G_q, which virtually eliminates erg currents. Constitutively active G_q produced a similarly strong block of M-current in published experiments (Haley *et al.* 1998; Suh *et al.* 2004). In parallel experiments with PLC-PH-EGFP, an optical probe for PIP_2 and IP_3, we found the expression of constitutively active G_q, caused all of the probe to leave the plasma membrane, as if all of the cellular PIP_2 had been depleted during many hours of G_q activity (Suh *et al.* 2004).

Why is the muscarinic suppression of erg only partial? Quick desensitization of the muscarinic receptor or a limiting factor upstream of PLC is unlikely, as KCNQ2/3 inhibition and PLC-PH-EGFP probe translocation in response to oxo-M in the same cell type are sustained over a similar time period of at least 3 min (Suh & Hille, 2002; Suh *et al.* 2004). Unfortunately we could not test the involvement of PLC directly, because both the PLC inhibitor U73122 and its 'inactive' analogue U73343 blocked erg current in our cells. Muscarinic suppression of erg may be incomplete because with muscarinic stimulation some step downstream of PLC (e.g. PIP_2 hydrolysis) does not proceed as completely as it does after 1 day of constitutively active G_q expression. Alternatively, the population of channels may be in a mixed state (e.g. of phosphorylation) only some of which can be modulated by oxo-M. Finally, full modulation of all channels may cause the partial effect that we observe.

One report concludes that Rho GTPase mediates TRH inhibition of erg via G_{13} (Storey *et al.* 2002). The evidence was: expression of constitutively active Rho nearly eliminated erg currents in GH_4C_1 cells; exposure to C3 toxin or expression of dominant-negative Rho reduced TRH action; and, as we found, expression of constitutively active G_{13} (one of the G proteins that can activate Rho) partially reduces erg currents. However, recent negative work with Rho kinase inhibitors did not corroborate this suggestion for TRH (Gómez-Varela *et al.* 2003). We did not find a block of muscarinic inhibition with C3 toxin, and we found that dominant-negative G_q was more effective at reducing muscarinic inhibition of erg than dominant-negative G_{13} in our tsA cells. In embryonic fibroblasts, both $G_{q/11}$ and $G_{12/13}$ are able to activate Rho signalling (Vogt *et al.* 2003). Thus, it is possible that M_1 receptors might activate a Rho pathway via G_q; nevertheless, that pathway does not seem essential for muscarinic inhibition.

Kinases

The literature suggests that erg/HERG channels are subject to several forms of inhibitory modulation. Pharmacological stimulation of several protein kinases and inhibition of others will reduce current. Thus, inhibitors of src kinase, and activators of PKC or PKA are all said to reduce currents (Barros *et al.* 1998; Cayabyab

& Schlichter, 2002; Wei *et al.* 2002). In one scenario, functional erg1 channels exist as a coprecipitable complex with src tyrosine kinase and are constitutively tyrosine phosphorylated (Cayabyab & Schlichter, 2002). The pharmacological inhibition of tyrosine kinases decreases erg current, and the activation of src increases it. Indeed we too found reduction of erg current with genistein – although oxo-M remained fully effective at inhibiting the remaining current. In addition, inhibiting phosphatases with vanadate or with dephostatin did not prevent muscarinic inhibition of erg current in our work, indicating that tyrosine dephosphorylation is not *required*. Conversely, elevating cyclic AMP reduces currents and shifts activation in HERG channels expressed in *Xenopus* oocytes, but not after consensus sequences for phosphorylation by PKA are mutated (Thomas *et al.* 1999). Thus, direct phosphorylation by PKA appears to be an effective mimic of receptor-mediated inhibition. Still, the PKA inhibitor H-89 does not prevent TRH inhibition of erg (Schledermann *et al.* 2001). Finally, the phorbol ester PMA inhibits HERG and erg channels and shifts activation. This effect and the action of TRH are reported as being insensitive to bisindolylmaleimide I at 1 μM (Kiehn *et al.* 1998; Schledermann *et al.* 2001) but sensitive at 10 μM (Barros *et al.* 1998; Thomas *et al.* 2003), a concentration that would inhibit PKA ($IC_{50} = 2\ \mu$M) as well as PKC ($IC_{50} = 10$ nM). The action of PMA persists after all PKC consensus sites on HERG channels are mutated (Thomas *et al.* 2003) and has been variously interpreted as a PKC-mediated stimulation of phosphorylation by PKA (Kiehn *et al.* 1998) or as an action of PMA on DAG-binding sites of other molecules (Schledermann *et al.* 2001). In our system PMA did not shift the voltage dependence of activation. It would be useful to try a similar experiment on HERG channels lacking the consensus PKA sites. R-erg2, which lacks these sites, can be modulated by TRH (Schledermann *et al.* 2001). Unexpectedly, one paper concludes that PKC is not needed for the inhibition of erg, but rather for its recovery (Gómez-Varela *et al.* 2003).

Here we find that PMA and its inactive analogue 4αPMA attenuate muscarinic inhibition of erg1 current equally. There is no attenuation of oxo-M inhibition with 1 μM staurosporine or 1 μM bisindolylmaleimide I or in cells dialysed with 4 mM non-hydrolysable AMP-PCP. Especially because AMP-PCP does not prevent inhibition, we conclude that muscarinic *inhibition* can occur without any active kinases, although *recovery* could be affected by block of kinases, agreeing with Gómez-Varela *et al.* (2003). This interpretation is tempered by our finding that 1 μM calphostin C reduces muscarinic inhibition by about 40%, and it does not preclude significant possible roles of kinases in other forms of modulation of erg/HERG channels. The isolated effect of calphostin C is reminiscent of the recent report that calphostin C, but not bisindolylmaleimide I, lowers the sensitivity of the M_1R-mediated inhibition of KCNQ current (Hoshi *et al.* 2003). Alternatively, it is possible that calphostin C acts on a substrate other than PKC, such as another protein with a DAG-binding site, as shown for RasGRP (Lorenzo *et al.* 2000). We found that oxo-M caused a slightly increased shift in the voltage dependence of activation after pretreating with PMA, raising the possibility that PKC phosphorylation of the channel due to PMA allows more shift, and dephosphorylation due to calphostin C does the opposite. We also found a small enhancement of inhibition with bisindolylmaleimide I and with AMP-PCP, which could point to an inhibitory effect of PKC on susceptibility of erg channels to muscarinic suppression. In contrast to our results with AMP-PCP, the TRH modulation in GH_3 cells was diminished by an ATP analogue, suggesting that the TRH pathway might require phosphorylation by an unknown kinase (Barros *et al.* 1993).

Later stages of inhibition

Cell-attached patch experiments on GH_3/B_6 cells showed that inhibition of erg by TRH requires a diffusible second messenger (Schledermann *et al.* 2001). This inhibition in GH_3/B_6 cells and the muscarinic inhibition in tsA cells also require a minimum level of intracellular calcium (Bauer *et al.* 1990; this paper). However, we have shown that inhibition is preserved when the calcium concentration is strongly buffered at resting levels and most sources of calcium signals are blocked. Hence, calcium does not carry an obligatory signal. One member of the eag family, hEAG1, is modulated directly by Ca^{2+}–calmodulin at an identified binding domain (Schönherr *et al.* 2000), but erg channels do not share this sequence and we found no sensitivity to calmodulin constructs.

Both the diffusible second messenger and the need for a permissive level of Ca^{2+} are properties of inhibition of M-current by phospholipase-C-coupled receptors (Beech *et al.* 1991; Cruzblanca *et al.* 1998; Shapiro *et al.* 2000). There, the need for calcium can be interpreted as reflecting the calcium requirement of phospholipase C-β in the hydrolysis of PIP_2 (see Ryu *et al.* 1987), and the depletion of PIP_2 is believed to cause M-current channels to close (Suh & Hille, 2002; Zhang *et al.* 2003; Ford *et al.* 2003). Virtually the same PIP_2-dependent model has been proposed by Bian *et al.* (2001) for modulation of HERG channels. These authors report a rapid decrease of HERG current with anti-PIP_2 antibodies included in the pipette in whole-cell mode, and an increase of current with PIP_2 included in the pipette in whole-cell mode. They also reported a decrease of rundown when PIP_2 was applied to the cytoplasmic face of an excised patch. A recent paper reports a shift of HERG activation towards hyperpolarized potentials after 10 min dialysis with PIP_2 in the pipette, which could be prevented by PIP_2 antibody (Wang *et al.* 2004). Both papers show a negative shift in voltage dependence but differ in that

an increase of maximal outward current with PIP_2 and a rundown with PIP_2 antibodies were seen by Bian *et al.* (2001) and not by Wang *et al.* (2004). Our own work finds no change with inclusion of either PIP_2 or PIP_2 antibodies in the pipette, but we lacked a positive control to verify the activity and effective dialysis of our reagents. Indeed when we tried the same kind of experiment with these PIP_2 or PIP_2 antibody solutions on KCNQ2/3 current, we also failed to observe any effects (data not shown). This issue cannot be regarded as resolved. Judging from the range of ideas in the literature, there could well be multiple types of modulation of these channels. The PIP_2 hypothesis seems viable, as do several other hypotheses. One of the difficulties in unravelling the mechanism pharmacologically may be that a single stimulus brings into play several mechanisms acting in parallel.

Recovery from inhibition

For KCNQ2/3 currents, analysis of recovery from inhibition was invaluable in showing that the channel required PIP_2 resynthesis to restore activity. There recovery needed active PI 4-kinase and ATP. For example, recovery of KCNQ2/3 currents was totally stopped by ATP-free pipette solutions or by high concentrations of wortmannin (50 μM) (Suh & Hille, 2002; Zhang *et al.* 2003; Ford *et al.* 2003). Unfortunately, recovery of erg current after muscarinic inhibition was weak and variable: on average it did not exceed 29% after 3 min. The inconsistency, the small recovery, and the small initial inhibition with a background of current rundown made analysis of recovery of erg less reliable. Some of our experiments would be consistent with the PIP_2 hypothesis. Recovery of erg was significantly slowed by 50 μM wortmannin when compared to 1 μM wortmannin; recovery may have been slowed by an ATP-free pipette solution; and rundown was speeded by both of these conditions. However, adding PIP_2 or PIP_2 antibodies to the pipette had no significant effects.

If erg channels do require PIP_2, then perhaps they bind it more tightly than KCNQ2/3 channels do. High affinity would mean that PIP_2 would have to fall to very low levels before erg is inhibited, consistent with a muscarinic inhibition that is weaker and slower to develop than inhibition of KCNQ2/3 current in the same cells (Suh & Hille, 2002) and inhibition would become total with prolonged expression of constitutively active G_q. In the simplest case, this scenario would predict that erg current would recover faster and more completely than KCNQ2/3 current. Since this is definitely not the case, even if PIP_2 might be an important variable, other players must also be invoked. An alternative scenario might be that erg channels can bind several acidic phospholipids and that depletion of PIP_2, PIP, and even PI will affect their activity. Then one might expect that muscarinic inhibition and recovery are slower than for KCNQ2/3 and only complete after hours of constitutively active G_q.

Conclusions

Two points about modulation of erg/HERG channels seem remarkable. One is that there are many different effective stimuli and pharmacological interventions, which suggest many alternative underlying mechanisms. The second is that, although each cell type or expression system differs in details, the overall biophysical phenomenology in each report is quite similar. Whatever the stimulus, there tends to be some reduction of maximum available current, a positive shift of the activation curve, acceleration of deactivation, and little effect on inactivation. In some cell types and with some stimuli one effect may be more prominent than the other. Thus, in this paper, the mean shift of erg1 activation by muscarinic stimulation was only 5 mV and the depression of maximum current was 30%, whereas with GH_3/B_6 cells and TRH as the stimulus the shift was 15 mV and the depression only 12% (Schledermann *et al.* 2001). In CHO cells and neuroblastoma cells, M_1-muscarinic stimulation caused a more marked increase in deactivation kinetics than we saw in tsA cells (Selyanko *et al.* 1999). Nevertheless, the similarities seem more impressive than the differences. One quite general interpretation would then be that the modulation(s) destabilize the open states and facilitate the closing transitions so that the microscopic open time becomes shorter. This could lead quite naturally to all of the changes above. There could of course be multiple ways to modify and inhibit erg/HERG channels.

Is there a physiological role of muscarinic inhibition of erg current? The mRNAs from the three erg channels that have been cloned so far (HERG: Warmke & Ganetzky, 1994; r-erg2 and r-erg3: Shi *et al.* 1997) are expressed in a variety of tissues and brain regions (Saganich *et al.* 2001; Papa *et al.* 2003). The distribution of erg1 protein in the central nervous system has also been described (Papa *et al.* 2003). Recent electrophysiological studies found erg current in neurones of some of these regions (Sacco *et al.* 2003; Schwarz *et al.* 2003). Because in some of these regions the M_1R has been found as well, e.g. in the Purkinje cells of the cerebellum (Tayebati *et al.* 2001) and in the hippocampus (Shiozaki *et al.* 2001), it is likely that muscarinic modulation of erg current contributes to the control of neuronal excitability. Since all three erg channels can be modulated by the TRH receptor (Schledermann *et al.* 2001), it is likely that erg2 and erg3 also are modulated by M_1R. As has been shown for hormonal secretion in pituitary lactotropes (Bauer *et al.* 1999), insulin secretion in pancreatic β-cells may also be influenced by modulation of erg current by the M_3- or even M_1-receptor (Rosati *et al.* 2000; Iismaa *et al.* 2000). Muscarinic modulation of erg currents might regulate neuronal excitability in the brain. Since various drugs of abuse as well as other

psychopharmacological drugs are known to inhibit erg current, they should destabilize the resting membrane potential and increase neuronal excitability.

References

Barros F, Gómez-Varela D, Viloria CG, Palomero T, Giráldez T & de la Peña P (1998). Modulation of human erg K^+ channel gating by activation of a G protein-coupled receptor and protein kinase C. *J Physiol* **511**, 333–346.

Barros F, Mieskes G, del Camino D & de la Peña P (1993). Protein phosphatase 2A reverses inhibition of inward rectifying K^+ currents by thyrotropin-releasing hormone in GH_3 pituitary cells. *FEBS Lett* **336**, 433–439.

Bauer CK, Meyerhof W & Schwarz JR (1990). An inward-rectifying K^+ current in clonal rat pituitary cells and its modulation by thyrotrophin-releasing hormone. *J Physiol* **429**, 169–189.

Bauer CK, Schäfer R, Schiemann D, Reid G, Hanganu I & Schwarz JR (1999). A functional role of the erg-like inward-rectifying K^+ current in prolactin secretion from rat lactotrophs. *Mol Cell Endocrinol* **148**, 37–45.

Bauer CK & Schwarz JR (2001). Physiology of EAG K^+ channels. *J Membr Biol* **182**, 1–15.

Beech DJ, Bernheim L, Mathie A & Hille B (1991). Intracellular Ca^{2+} buffers disrupt muscarinic suppression of Ca^{2+} current and M current in rat sympathetic neurons. *Proc Natl Acad Sci U S A* **88**, 652–656.

Bernheim L, Beech DJ & Hille B (1991). A diffusible second messenger mediates one of the pathways coupling receptors to calcium channels in rat sympathetic neurons. *Neuron* **6**, 859–867.

Bernstein LS, Ramineni S, Hague C, Cladman Chidiac P, Levey AI & Hepler JR (2004). RGS2 binds directly and selectively to the M_1 muscarinic acetylcholine receptor third intracellular loop to modulate $G_{q/11}\alpha$ signaling. *J Biol Chem* **279**, 21248–21256.

Berstein G, Blank JL, Smrcka AV, Higashijima T, Sternweis PC, Exton JH & Ross EM (1992). Reconstitution of agonist-stimulated phosphatidylinositol 4,5-bisphosphate hydrolysis using purified m1 muscarinic receptor, $G_{q/11}$, and phospholipase C-β1. *J Biol Chem* **267**, 8081–8088.

Bian J, Cui J & McDonald TV (2001). HERG K^+ channel activity is regulated by changes in phosphatidyl inositol 4,5-bisphosphate. *Circ Res* **89**, 1168–1176.

Cayabyab FS & Schlichter LC (2002). Regulation of an ERG K^+ current by Src tyrosine kinase. *J Biol Chem* **277**, 13673–13681.

Cayabyab FS, Tsui FW & Schlichter LC (2002). Modulation of the ERG K^+ current by the tyrosine phosphatase, SHP-1. *J Biol Chem* **277**, 48130–48138.

Cruzblanca H, Koh DS & Hille B (1998). Bradykinin inhibits M current via phospholipase C and Ca^{2+} release from IP_3-sensitive Ca^{2+} stores in rat sympathetic neurons. *Proc Natl Acad Sci U S A* **95**, 7151–7156.

Curran ME, Splawski I, Timothy KW, Vincent GM, Green ED & Keating MT (1995). A molecular basis for cardiac arrhythmia: HERG mutations cause long QT syndrome. *Cell* **80**, 795–803.

Ehrlich JR, Pourrier M, Weerapura M, Ethier N, Marmabachi M, Hebert TE & Nattel S (2004). KvLQT1 modulates the distribution and biophysical properties of HERG: a novel alpha–subunit interaction between delayed-rectifier currents. *J Biol Chem* **279**, 1233–1241.

Ford CP, Stemkowski PL, Light PE & Smith PA (2003). Experiments to test the role of phosphatidylinositol 4,5-bisphosphate in neurotransmitter-induced M-channel closure in bullfrog sympathetic neurons. *J Neurosci* **23**, 4931–4941.

Gamper N & Shapiro MS (2003). Calmodulin mediates Ca^{2+}-dependent modulation of M-type K^+ channels. *J General Physiol* **122**, 17–31.

Garcia DE, Brown S, Hille B & Mackie K (1998). Protein kinase C disrupts cannabinoid actions by phosphorylation of the CB1 cannabinoid receptor. *J Neurosci* **18**, 2834–2841.

Geiser JR, van Tuinen D, Brockerhoff SE, Neff MM & Davis TN (1991). Can calmodulin function without binding calcium? *Cell* **65**, 949–959.

Gómez-Varela D, Giráldez T, de la Peña P, Dupuy SG, García-Manso D & Barros F (2003). Protein kinase C is necessary for recovery from the thyrotropin-releasing hormone-induced r-ERG current reduction in GH_3 rat anterior pituitary cells. *J Physiol* **547**, 913–929.

Gullo F, Ales E, Rosati B, Lecchi M, Masi A, Guasti L, Cano-Abad MF, Arcangeli A, Lopez MG & Wanke E (2003). ERG K^+ channel blockade enhances firing and epinephrine secretion in rat chromaffin cells: the missing link to LQT2-related sudden death? *FASEB J* **17**, 330–332.

Haley JE, Abogadie FC, Delmas P, Dayrell M, Vallis Y, Milligan G, Caulfield MP, Brown DA & Buckley NJ (1998). The α subunit of G_q contributes to muscarinic inhibition of the M-type potassium current in sympathetic neurons. *J Neurosci* **18**, 4521–4531.

Haley JE, Delmas P, Offermanns S, Abogadie FC, Simon MI, Buckley NJ & Brown DA (2000). Muscarinic inhibition of calcium current and M current in $G\alpha_q$-deficient mice. *J Neurosci* **20**, 3973–3979.

Heximer SP, Watson N, Linder ME, Blumer KJ & Hepler JR (1997). RGS2/G0S8 is a selective inhibitor of Gqα function. *Proc Natl Acad Sci U S A* **94**, 14389–14393.

Higashida H, Brown DA & Robbins J (2000). Both linopirdine- and WAY123,398-sensitive components of $I_{K(M,ng)}$ are modulated by cyclic ADP ribose in NG108-15 cells. *Pflugers Arch* **441**, 228–234.

Hilgemann DW, Feng S & Nasuhoglu C (2001). The complex and intriguing lives of PIP_2 with ion channels and transporters. *Sci STKE* **2001**, RE19.

Hoshi N, Zhang JS, Omaki M, Takeuchi T, Yokoyama S, Wanaverbecq N, Langeberg LK, Yoneda Y, Scott JD, Brown DA & Higashida H (2003). AKAP150 signaling complex promotes suppression of the M-current by muscarinic agonists. *Nat Neurosci* **6**, 564–571.

Iismaa TP, Kerr EA, Wilson JR, Carpenter L, Sims N & Biden TJ (2000). Quantitative and functional characterization of muscarinic receptor subtypes in insulin-secreting cell lines and rat pancreatic islets. *Diabetes* **49**, 392–398.

Just I, Hofmann F, Genth H & Gerhard R (2001). Bacterial protein toxins inhibiting low-molecular-mass GTP-binding proteins. *Int J Med Microbiol* **291**, 243–250.

Karle CA & Kiehn J (2002). An ion channel 'addicted' to ether, alcohol and cocaine: the HERG potassium channel. *Cardiovasc Res* **53**, 6–8.

Kiehn J, Karle C, Thomas D, Yao X, Brachmann J & Kubler W (1998). HERG potassium channel activation is shifted by phorbol esters via protein kinase A-dependent pathways. *J Biol Chem* **273**, 25285–25291.

Kiehn J, Wible B, Ficker E, Taglialatela M & Brown AM (1995). Cloned human inward rectifier K^+ channel as a target for class III methanesulfonanilides. *Circ Res* **77**, 1151–1155.

Lang P, Guizani L, Vitte-Mony I, Stancou R, Dorseuil O, Gacon G & Bertoglio J (1992). ADP-ribosylation of the ras-related, GTP-binding protein RhoA inhibits lymphocyte-mediated cytotoxicity. *J Biol Chem* **267**, 11677–11680.

Lanzafame AA, Christopoulos A & Mitchelson F (2003). Cellular signaling mechanisms for muscarinic acetylcholine receptors. *Receptors Channels* **9**, 241–260.

Lorenzo PS, Beheshti M, Pettit GR, Stone JC & Blumberg PM (2000). The guanine nucleotide exchange factor RasGRP is a high-affinity target for diacylglycerol and phorbol esters. *Mol Pharmacol* **57**, 840–846.

Marrion NV (1997). Control of M-current. *Annu Rev Physiol* **59**, 483–504.

Mathie A, Bernheim L & Hille B (1992). Inhibition of N- and L-type calcium channels by muscarinic receptor activation in rat sympathetic neurons. *Neuron* **8**, 907–914.

Melliti K, Meza U & Adams BA (2001). RGS2 blocks slow muscarinic inhibition of N-type Ca^{2+} channels reconstituted in a human cell line. *J Physiol* **532**, 337–347.

Meves H, Schwarz JR & Wulfsen I (1999). Separation of M-like current and ERG current in NG108-15 cells. *Br J Pharmacol* **127**, 1213–1223.

Papa M, Boscia F, Canitano A, Castaldo P, Sellitti S, Annunziato L & Taglialatela M (2003). Expression pattern of the ether-a-go-go-related (ERG) K^+ channel-encoding genes ERG1, ERG2, and ERG3 in the adult rat central nervous system. *J Comp Neurol* **466**, 119–135.

Rampe D, Murawsky MK, Grau J & Lewis EW (1998). The antipsychotic agent sertindole is a high affinity antagonist of the human cardiac potassium channel HERG. *J Pharmacol Exp Ther* **286**, 788–793.

Rosati B, Marchetti P, Crociani O, Lecchi M, Lupi R, Arcangeli A, Olivotto M & Wanke E (2000). Glucose- and arginine-induced insulin secretion by human pancreatic β-cells: the role of HERG K^+ channels in firing and release. *FASEB J* **14**, 2601–2610.

Runnels LW, Yue L & Clapham DE (2002). The TRPM7 channel is inactivated by PIP_2 hydrolysis. *Nat Cell Biol* **4**, 329–336.

Ryu SH, Cho KS, Lee KY, Suh PG & Rhee SG (1987). Purification and characterization of two immunologically distinct phosphoinositide-specific phospholipases C from bovine brain. *J Biol Chem* **262**, 12511–12518.

Sacco T, Bruno A, Wanke E & Tempia F (2003). Functional roles of an ERG current isolated in cerebellar Purkinje neurons. *J Neurophysiol* **90**, 1817–1828.

Saganich MJ, Machado E & Rudy B (2001). Differential expression of genes encoding subthreshold-operating voltage-gated K^+ channels in brain. *J Neurosci* **21**, 4609–4624.

Sanguinetti MC, Jiang C, Curran ME & Keating MT (1995). A mechanistic link between an inherited and an acquired cardiac arrhythmia: HERG encodes the I_{Kr}. *Cell* **81**, 299–307.

Satoh H (2002). Modulation by nicotine of the ionic currents in guinea pig ventricular cardiomyocytes. Relatively higher sensitivity to I_{Kr} and I_{Kl}. *Vascul Pharmacol* **39**, 55–61.

Schledermann W, Wulfsen I, Schwarz JR & Bauer CK (2001). Modulation of rat erg1, erg2, erg3 and HERG K^+ currents by thyrotropin-releasing hormone in anterior pituitary cells via the native signal cascade. *J Physiol* **532**, 143–163.

Schönherr R, Löber K & Heinemann SH (2000). Inhibition of human *ether à go-go* potassium channels by Ca^{2+}/calmodulin. *EMBO J* **19**, 3263–3271.

Schwarz JR, Schweizer M, Schuricht K, Schledermann W & Glassmeier G (2003). Erg potassium channels in rat nucleus raphe neurons. *Program No. 53.7 2003 Abstract Viewer/Itinerary Planner*. Society for Neuroscience, Washington, DC, USA.

Selyanko AA, Hadley JK, Wood IC, Abogadie FC, Delmas P, Buckley NJ, London B & Brown DA (1999). Two types of K^+ channel subunit, Erg1 and KCNQ2/3, contribute to the M-like current in a mammalian neuronal cell. *J Neurosci* **19**, 7742–7756.

Shapiro MS, Roche JP, Kaftan EJ, Cruzblanca H, Mackie K & Hille B (2000). Reconstitution of muscarinic modulation of the KCNQ2/KCNQ3 K^+ channels that underlie the neuronal M current. *J Neurosci* **20**, 1710–1721.

Shapiro MS, Wollmuth LP & Hille B (1994). Modulation of Ca^{2+} channels by PTX-sensitive G-proteins is blocked by N-ethylmaleimide in rat sympathetic neurons. *J Neurosci* **14**, 7109–7116.

Shapiro MS, Zhou J & Hille B (1996). Selective disruption by protein kinases of G-protein-mediated Ca^{2+} channel modulation. *J Neurophysiol* **76**, 311–320.

Shi W, Wymore RS, Wang HS, Pan Z, Cohen IS, McKinnon D & Dixon JE (1997). Identification of two nervous system-specific members of the *erg* potassium channel gene family. *J Neurosci* **17**, 9423–9432.

Shibasaki T (1987). Conductance and kinetics of delayed rectifier potassium channels in nodal cells of the rabbit heart. *J Physiol* **387**, 227–250.

Shiozaki K, Iseki E, Hino H & Kosaka K (2001). Distribution of m1 muscarinic acetylcholine receptors in the hippocampus of patients with Alzheimer's disease and dementia with Lewy bodies – an immunohistochemical study. *J Neurol Sci* **193**, 23–28.

Storey NM, O'Bryan JP & Armstrong DL (2002). Rac and Rho mediate opposing hormonal regulation of the ether-a-go-go-related potassium channel. *Curr Biol* **12**, 27–33.

Suh BC & Hille B (2002). Recovery from muscarinic modulation of M current channels requires phosphatidylinositol 4,5-bisphosphate synthesis. *Neuron* **35**, 507–520.

Suh BC, Horowitz LF, Hirdes W, Mackie K & Hille B (2004). Regulation of KCNQ2/KCNQ3 current by G protein cycling: the kinetics of receptor-mediated signaling by G_q. *J Gen Physiol* **123**, 663–683.

Tayebati SK, Vitali D, Scordella S & Amenta F (2001). Muscarinic cholinergic receptors subtypes in rat cerebellar cortex: light microscope autoradiography of age-related changes. *Brain Res* **889**, 256–259.

Thomas D, Zhang W, Karle CA, Kathöfer S, Schols W, Kubler W & Kiehn J (1999). Deletion of protein kinase A phosphorylation sites in the HERG potassium channel inhibits activation shift by protein kinase A. *J Biol Chem* **274**, 27457–27462.

Thomas D, Zhang W, Wu K, Wimmer AB, Gut B, Wendt-Nordahl G, Kathöfer S, Kreye VA, Katus HA, Schoels W, Kiehn J & Karle CA (2003). Regulation of HERG potassium channel activation by protein kinase C independent of direct phosphorylation of the channel protein. *Cardiovasc Res* **59**, 14–26.

Tristani-Firouzi M & Sanguinetti MC (2003). Structural determinants and biophysical properties of HERG and KCNQ1 channel gating. *J Mol Cell Cardiol* **35**, 27–35.

Trudeau MC, Warmke JW, Ganetzky B & Robertson GA (1995). HERG, a human inward rectifier in the voltage-gated potassium channel family. *Science* **269**, 92–95.

Vogt S, Grosse R, Schultz G & Offermanns S (2003). Receptor-dependent RhoA activation in G_{12}/G_{13}-deficient cells: genetic evidence for an involvement of G_q/G_{11}. *J Biol Chem* **278**, 28743–28749.

Wang J, Zhang Y, Wang H, Han H, Nattel S, Yang B & Wang Z (2004). Potential mechanisms for the enhancement of HERG K^+ channel function by phospholipid metabolites. *Br J Pharmacol* **141**, 586–599.

Warmke JW & Ganetzky B (1994). A family of potassium channel genes related to *eag. Drosophila* and mammals. *Proc Natl Acad Sci U S A* **91**, 3438–3442.

Wei Z, Thomas D, Karle CA, Kathöfer S, Schenkel J, Kreye VA, Ficker E, Wible BA & Kiehn J (2002). Protein kinase A-mediated phosphorylation of HERG potassium channels in a human cell line. *Chin Med J* **115**, 668–676.

Wymore RS, Gintant GA, Wymore RT, Dixon JE, McKinnon D & Cohen IS (1997). Tissue and species distribution of mRNA for the I_{Kr}-like K^+ channel, *erg. Circ Res* **80**, 261–268.

Zhang H, Craciun LC, Mirshahi T, Rohacs T, Lopes CM, Jin T & Logothetis DE (2003). PIP_2 activates KCNQ channels, and its hydrolysis underlies receptor-mediated inhibition of M currents. *Neuron* **37**, 963–975.

Zhou Z, Vorperian VR, Gong Q, Zhang S & January CT (1999). Block of HERG potassium channels by the antihistamine astemizole and its metabolites desmethylastemizole and norastemizole. *J Cardiovasc Electrophysiol* **10**, 836–843.

Acknowledgements

This work was supported by National Institute of Health Grants NS08174, NS07332 and DA11322. We would like to thank Lea Miller for technical assistance, Ken Mackie for help with molecular biology, J. P. Johnson, Byung-Chang Suh, Jürgen R. Schwarz, and Christiane K. Bauer for commenting on a draft of the paper, and Paulette Brunner for help with confocal microscopy in the Keck Center.